ACS OMEGA

Open Access

http://pubs.acs.org/journal/acsodf

Article

Fluorescently Modified NDM-1: A Versatile Drug Sensor for Rapid *In Vitro* β-Lactam Antibiotic and Inhibitor Screening

Sai-Fung Chung,[#] Suet-Ying Tam,[#] Wai-Ting Wong, Pui-Kin So, Wing-Lam Cheong, Chun-Wing Mak, Leo Man-Yuen Lee, Pak-Ho Chan, Kwok-Yin Wong,* and Yun-Chung Leung*

Cite This: *ACS Omega* 2024, 9, 9161−9169

Read Online

ACCESS | Metrics & More | Article Recommendations | Supporting Information

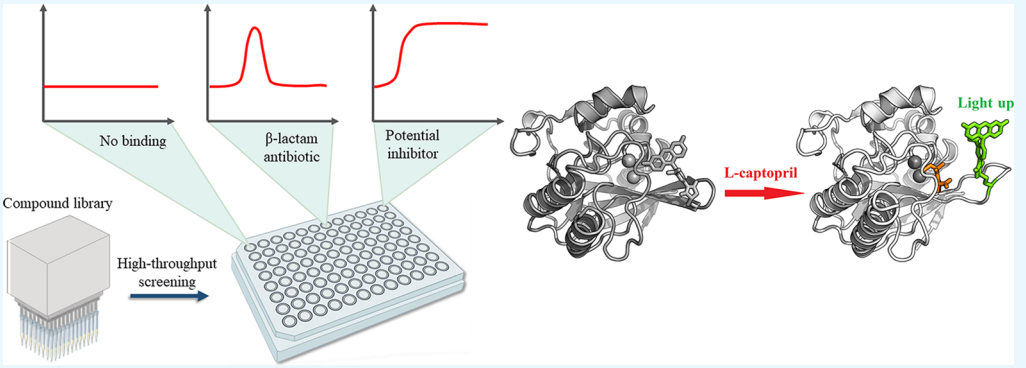

ABSTRACT: We successfully developed a fluorescent drug sensor from clinically relevant New Delhi metallo-β-lactamase-1 (NDM-1). The F70 residue was chosen to be replaced with a cysteine for conjugation with thiol-reactive fluorescein-5-maleimide to form fluorescent F70Cf, where "f" refers to fluorescein-5-maleimide. Our proteolytic studies of unlabeled F70C and labeled F70Cf monitored by electrospray ionization−mass spectrometry (ESI-MS) revealed that fluorescein-5-maleimide was specifically linked to C70 in 1:1 mole ratio (F70C:fluorophore). Our drug sensor (F70Cf) can detect the β-lactam antibiotics cefotaxime and cephalothin by giving stronger fluorescence in the initial binding phase and then declining fluorescence signals as a result of the hydrolysis of the antibiotics into acid products. F70Cf can also detect non-β-lactam inhibitors (e.g., L-captopril, D-captopril, DL-thiorphan, and thanatin). In all cases, F70Cf exhibits stronger fluorescence due to inhibitor binding and subsequently sustained fluorescence signals in a later stage. Native ESI-MS results show that F70Cf can bind to all four inhibitors. Moreover, our drug sensor is compatible with a high-throughput microplate reader and has the capability to perform *in vitro* drug screening.

INTRODUCTION

Since the discovery of β-lactam antibiotics, they have been widely used in antimicrobial chemotherapies.[1] The overuse and sometimes abuse of β-lactam antibiotics, however, have led to the increasing emergence of antibiotic-resistant bacteria capable of producing β-lactamases to destroy β-lactam antibiotics through efficient β-lactam hydrolysis (Scheme 1),[2] thus making the β-lactam ring-opened antibiotics no longer able to inhibit penicillin-binding proteins (PBPs) in bacteria to build cell walls for survival.[3]

To date, more than 400 clinically relevant β-lactamases have been identified. Such bacterial enzymes can efficiently open the four-membered β-lactam ring through hydrolysis, thus making the antibiotics clinically inactive (i.e., unable to bind to PBPs).[4] β-Lactamases can be classified into four classes according to their amino acid sequences: classes A−D.[5] In general, the hydrolytic action of β-lactamases is presented by the following catalytic pathway (Scheme 2).[6,7]

Class A, C, and D β-lactamases are serine-type β-lactamases; they cleave the β-lactam ring by forming a covalent linkage between the −OH group of serine within the enzyme's active site and the β-lactam carbonyl group through acylation. Class B β-lactamases are metallo-β-lactamases (MBLs) that are dependent on two Zn(II) ions to initiate the reactions.[8] The

Scheme 1. β-Lactam Hydrolysis by β-Lactamase

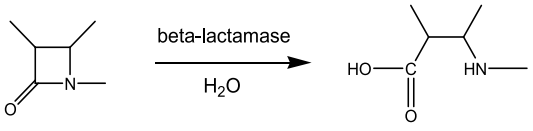

Received: October 16, 2023
Revised: January 14, 2024
Accepted: January 25, 2024
Published: February 13, 2024

https://doi.org/10.1021/acsomega.3c08117
ACS Omega 2024, 9, 9161−9169

Scheme 2. Catalytic Pathway of β-Lactamases toward β-Lactam Antibiotics

$$E + S \leftrightarrow ES \rightarrow ES^* \rightarrow E + P$$

where E is the free enzyme (β-lactamase), S is the substrate (β-lactam antibiotic), ES is the non-covalent enzyme−substrate complex, ES* is the covalent enzyme−substrate complex, and P is the carboxylic acid product.

New Delhi metallo-β-lactamase 1 (NDM-1) is one of the carbapenemases produced by carbapenem-resistant Enterobacteriaceae.[2] It can hydrolyze a wide range of β-lactam antibiotics, including carbapenems,[9] and most β-lactamase antibiotics (except for monobactams).[10] More worryingly, changes of amino acids through gene mutations in NDM-1 have resulted in the notorious NDM family containing various NDM-type β-lactamase variants with different substrate and kinetic profiles.[11−13] Thus, bacteria acquiring NDM-type β-lactamases represent a major threat to human health and are generally regarded as "superbugs" because only limited antibiotics are available for treating such bacteria.[1] To the best of our knowledge, there is currently no clinically useful NDM-1 inhibitor against NDM-1 in the past decades.[1,14]

Because of their serious threat to human health,[15] there is an urgent need for searching potent drugs against NDM-type β-lactamases. To this end, effective drug sensors based on NDM-type β-lactamases must be available for the discovery of new drug candidates and for antibiotic/inhibitor screening *in vitro*. NDM-1 is regarded as the ancestor of members in the NDM family and shares a common tertiary structure to other NDM-type β-lactamases.[14,16] Thus, NDM-1 represents an excellent protein model to develop a fluorescent drug sensor (by attaching a thiol-reactive fluorophore to a cysteine at the active site)[17] for studying its ability to perform drug discovery and antibiotic/inhibitor screening *in vitro*. More importantly, such information is particularly crucial for extending the development of tailor-made fluorescent drug sensors based on clinically relevant NDM-type variants to speed up future drug design and development as well as *in vitro* drug screening.

The wild-type NDM-1 β-lactamase itself has a cysteine residue at the 208th position, which is responsible for binding to Zn^{2+} for catalyzing the hydrolysis of β-lactam antibiotics.[18] C208 is buried within the active site such that fluorophore labeling at C208 is more difficult due to its binding to Zn^{2+} and the buried environment around C208. These structural properties largely prevents unwanted labeling C208 with a thiol-reactive fluorophore at C208, which would otherwise lead to the loss of the hydrolytic activity of NDM-1.[19] We reasoned that if we replaced an amino acid (more exposed) close to the active site with a cysteine and then attached the cysteine residue to a thiol-reactive fluorophore, the fluorophore can be specifically attached to the chosen cysteine residue and fluorescently sense the binding of antibiotics/inhibitors.[20−25] We replaced F70 with a cysteine and then labeled it with thiol-reactive fluorescein-5-maleimide in a carefully adjusted 1:1.3 mole ratio (to avoid nonspecific conjugation at C208) to form fluorescent F70Cf. F70 was chosen for replacement with a cysteine because (1) F70 (more exposed) lies close to the active site and, therefore, attaching F70 with the fluorescein label is likely to detect antibiotic/inhibitor binding, and (2) F70 is highly conserved in the NDM family[13,16] and, therefore, construction of a class of fluorescent NDM variants as drug sensors becomes feasible. The entry and leaving of β-lactam antibiotics/inhibitors can cause the fluorescein label to move in and out of the active site (which is relatively hydrophobic and may contain amino acid quenchers). Such subtle movements can induce the fluorescein label to give fluorescence changes in response to drug binding.

MATERIALS AND METHODS

Materials. L-Arginine, DL-thiorphan, L-captopril, and kanamycin were obtained from Sigma-Aldrich (St. Louis, MO). Thanatin (GSKKPVPIIYCNRRTGKCQRM) was purchased from GL Biochem (Shanghai, CN). D-Captopril was purchased from TLC Pharmaceutical Standards (Pony Dr, CA). Fluorsecein-5-maleimide was obtained from Invitrogen (Carlsbad, CA, USA).

Expression Vector Cloning and Mutation. The NDM-1 sequence was cloned into a pET-3k vector (a modified pET-3a vector with the replacement of ampicillin by kanamycin). The NDM-1 mutant (F70C) was constructed by the replacement of phenylalanine located at the 70th position by a cysteine using the QuikChange Site-Directed Mutagenesis Kit (Stratagene, CA, USA). The mutagenic forward and reverse primers are 5′ GAC ATG CCG GGT TGC GGG GCA GTC GCT TCC 3′ and 5′ GGA AGC GAC TGC CCC GCA ACC CGG CAT GTC 3′, respectively.

Recombinant Protein Expression and Purification. For protein expression, a single colony of *Escherichia coli* BL21(DE3) inserted with a designed vector was incubated into 10 mL of Lysogeny broth (LB) medium with 50 μg/mL kanamycin and cultured at 30 °C with shaking at 250 rpm overnight. Two milliliters of this LB medium was transferred into 200 mL of LB medium. When the OD_{600} of the culture reached 0.6, isopropylthiogalactoside (IPTG) with a final concentration of 0.2 mM was added and incubated at 16 °C at 250 rpm overnight.

For protein purification, to avoid any unwanted divalent metal ions, nickel(II) and cobalt(II) ions were inserted into metalloprotein NDM-1 during the purification process, which may affect the downstream assays. No purification tag including $(His)_6$-tagged is used. Cells were harvested by centrifugation at 8000 rpm at 4 °C for 30 min. The cell pellet was resuspended in lysis buffer (50 μM $ZnCl_2$ and 20 mM Tris−HCl buffer, pH 7.4) and lysed with an ultrasonic homogenizer (QSonica sonicators). The supernatant was harvested by centrifugation at 13,000 rpm at 4 °C for 1 h. The filtered supernatant was applied into the HiTrap Q HP (GE Healthcare) column with washing buffer (20 mM Tris−HCl buffer, pH 7.4) and elution buffer (1 M NaCl and 20 mM Tris−HCl buffer, pH 7.4). Impurities were removed in flow-through, and targeted proteins were collected in 10% elution. The targeted proteins were buffer-exchanged into a labeling buffer (50 μM $ZnCl_2$ and 20 mM Tris−HCl buffer, pH 7.0) and stored at −80 °C.

Enzyme Labeling (F70Cf). F70C enzymes were diluted into 1 mg/mL by labeling buffer. Different folds of molar excess (1:1.3 and 1:3) of fluorescein-5-maleimide were added to the enzyme solution. The mixtures were reacted at room temperature (22 °C) at different time points (from 30 min to 2 h). Amicon (MWCO = 10k Da) was used to remove excess dye using a labeling buffer. All labeled F70C (F70Cf) enzymes were stored at −80 °C.

Circular Dichroism (CD) Spectroscopic Analysis. A JASCO J-1500 Circular Dichroism Spectrophotometer was used to determine the secondary structure of F70C, F70Cf,

https://doi.org/10.1021/acsomega.3c08117
ACS Omega 2024, 9, 9161−9169

and wild-type NDM-1 under 10 mM potassium phosphate buffer at pH 7.5 with a final concentration of 5 μM. Each CD spectrum was collected from an average of 3 scans, and the CD signals were expressed as molar ellipticity (deg cm^2 dmol^{-1}).

Specific Activity. The specific activities (U/mg) of wild-type NDM-1, F70C, and F70Cf were measured by ultraviolet−visible spectroscopy. Enzymes (final concentration: 0.001 mg/mL) were incubated with 100 μM of different antibiotics, cefotaxime, ceftazidime, penicillin G, ampicillin, and Meropenem in 500 μL of buffer (50 μM $ZnCl_2$ and 20 mM Tris−HCl buffer, pH 7.0). Antibiotic hydrolysis was monitored at 264 nm (cefotaxime), 260 nm (ceftazidime), 240 nm (penicillin G), 235 nm (ampicillin), and 297 nm (Meropenem). The molar extinction coefficients were used as follows: cefotaxime = −7250 M^{-1} cm^{-1}, ceftazidime = −8660 M^{-1} cm^{-1}, penicillin G = −560 M^{-1} cm^{-1}, ampicillin = 900 M^{-1} cm^{-1}, and Meropenem = −10940 M^{-1} cm^{-1}.

Determination of Molecular Mass, Purity, and Labeling Efficiency. Liquid chromatography−electrospray ionization−mass spectrometry (LC-ESI-MS) experiments were performed with an Agilent 6540 QTOF mass spectrometer coupled with an Agilent 1290 Infinity UHPLC system. Purified wild-type NDM-1 enzymes, F70C enzymes, and labeled F70Cf enzymes were injected into a C4 LC column and eluted with a linear gradient from 95% solvent A:5% solvent B to 5% solvent A:95% solvent B, where solvent A was Milli-Q water and solvent B was acetonitrile, each with 0.1% formic acid. The mass spectrometer was operated in positive ion mode. ESI-MS data was acquired with an m/z range of 600−1600, from which multiply-charged mass spectra were obtained. The multiply-charged mass spectra were deconvoluted by the MassHunter BioConfirm program to obtain the molecular mass of proteins. The calculated molecular mass values of NDM-1 F70C and NDM-1 F70Cf are 25637 and 26064 Da, respectively.

Studies of the Interactions of Fluorescein-Labeled F70C Enzyme (F70Cf) with Inhibitors. The interactions of intact F70Cf and the inhibitors (L-arginine, L-captopril, D-captopril, DL-thiorphan, and thanatin) were detected by native ESI-MS on a Waters Synapt G2-Si Quadrupole-Ion Mobility-Time-of-flight Mass Spectrometer. Prior to ESI-MS analysis, the protein was buffer-exchanged into 20 mM ammonium acetate with 50 μM $ZnCl_2$ buffer with ultrafiltration devices. Equal volumes of F70Cf and inhibitors were mixed in a molar ratio of 1:20 for 10 min, and the mixture was directly loaded into metal-coated glass capillaries, which were subsequently mounted onto the nano-ESI source for MS analysis.

Determination of the Labeling Site on F70Cf. F70C and F70Cf enzymes were first buffer-exchanged into 50 mM ammonium bicarbonate, and subsequently, sequencing grade trypsin (Progema V5111) was added to the enzymes in a trypsin:enzyme ratio of 1:50 (w/w). Protease digestions were conducted at 37 °C for 16 h. Digested enzymes were analyzed by an Agilent 6540 QTOF mass spectrometer coupled to an Agilent 1290 Infinity UHPLC system. Peptides were separated and eluted in a C18 LC column with a linear gradient elution from 95% solvent A:5% solvent B to 5% solvent A:95% solvent B, where solvent A was Milli-Q water and solvent B was acetonitrile, each with 0.1% formic acid. Peptide assignment was performed with Agilent Masshunter-BioConfirm software.

Fluorescence Measurements. Fluorescence measurements for the detection of labeled F70C (F70Cf) inhibitors (L-captopril, D-captopril, DL-thiorphan and thanatin) were performed on an Agilent Cary Eclipse Fluorescence Spectrophotometer (Agilent). Time-course fluorescence measurements were recorded at 518 nm by exciting F70Cf (final concentration: 0.13 μM) at 494 nm with different concentrations of inhibitors arginine, D-captopril, L-captopril, DL-thiorphan, and thanatin (0, 2, 20, and 200 μM) in labeling buffer (50 μM $ZnCl_2$ and 20 mM Tris−HCl buffer, pH 7.0) in a quartz cuvette. Triplicate measurements were performed for each inhibitor.

For high-throughput inhibitor screening experiments, the fluorescence signal changes were recorded by adding 10 μL of each inhibitor (final concentration: 200 μM) automatically into 250 μL of F70Cf (final concentration: 0.13 μM) in a 96-well plate containing 50 μM $ZnCl_2$ and 20 mM Tris−HCl buffer (pH 7.0) using a Thermo Scientific Varioskan LUX Multimode Microplate Reader (Thermo Fisher Scientific) (n = 3). The excitation and emission wavelengths were 494 and 520 nm, respectively. The injection of each inhibitor was started at 0.5 min.

For the proteolytic study of F70Cf, the mass ratio of F70Cf and trypsin was 20 to 1 in 50 μM $ZnCl_2$ and 20 mM Tris−HCl buffer (pH 7.0). The fluorescence spectra of these trypsinized samples were recorded by excitation at 494 nm at various time intervals (after 0, 1, 3, 9, and 18 h of trypsinization) and recorded by an Agilent Cary Eclipse Fluorescence Spectrophotometer (Agilent) (n = 3 measurements).

RESULTS AND DISCUSSION

Protein Purification and Fluorophore Labeling. NDM-1 is a superbug enzyme that chelates two Zn^{2+} ions as cofactors. It can hydrolyze a wide range of β-lactam antibiotics in the world. To study the action of naturally occurring Zn^{2+} on β-lactam antibiotics and inhibitors, wild-type NDM-1 (with a molecular mass of 25681 Da, Figure S1c) and its mutant (F70C) without $(His)_6$-tags were produced to avoid any replacement of other divalent cations, such as Ni^{2+} and Co^{2+}, during purification.[26,27] The wild-type NDM-1 was mutated at the 70th amino acid (phenylalanine) into a cysteine residue for specific labeling with fluorescein-5-malemide (F5M) close to the active site. F70C (with a molecular mass of 25637 Da) was highly expressed in *E. coli* after the induction of IPTG (Figure S1a) in high purity by using an anion exchange column in a 10% elution buffer (Figure S1b). F70C shows a similar secondary structure (Figure S2) and specific activity as compared to the wild-type NDM-1 against different β-lactam antibiotics, indicating that the F70C mutation does not significantly weaken the activity as compared to wild-type NDM-1 (Table S1). A decrease in the activity of NDM-1 after labeling with F5M was observed since F5M at the active site hindered the hydrolytic activity of NDM-1 to some extent (Table S1). However, this did not affect the generation of fluorescence signal intensity upon NDM-1 binding to antibiotics and inhibitors.

After labeling F70C with F5M to become F70Cf (where "f" refers to fluorescein-5-maleimide), F70Cf shows fluorescence signals on a SDS-PAGE gel (Figure S3). To further confirm the attachment of F5M on F70C, the molecular mass of F70C before (25637 Da) and after (26064 Da) labeling was detected by electrospray−ionization mass spectrometry (ESI-MS). Since there are two cysteine residues in F70C (Figure 1; one is buried inside the active site (C208) and bound to Zn^{2+}, whereas the other (C70) lies close to the active site but with higher exposure to the external aqueous environment), it is important to optimize the fluorophore labeling ratio so as to

https://doi.org/10.1021/acsomega.3c08117
ACS Omega 2024, 9, 9161−9169

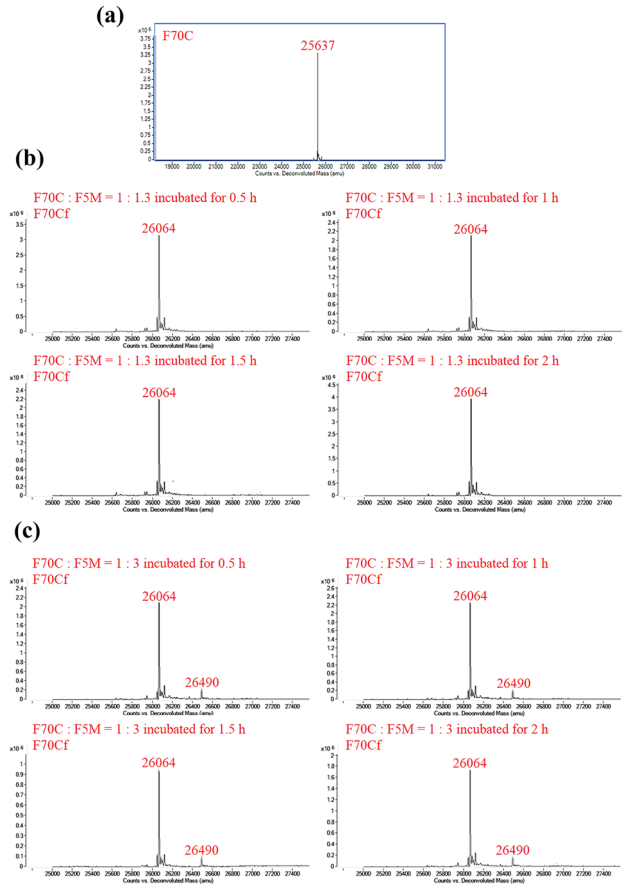

Figure 1. LC-ESI-MS spectra of F70C and F70Cf. (a) Molecular mass of F70C. (b) Molecular mass of F70Cf after incubating 1.3-fold molar excess of fluorescein-5-maleimide at different time intervals. (c) Molecular mass of F70Cf after incubating a 3-fold molar excess of fluorescein-5-maleimide at different time points.

avoid unwanted labeling at C208 (at the active site). We tried different mole ratios of F70C to F5M (1:1.3 and 1:3) and incubated them for different time intervals (Figure 1). We found that labeling F70C to F5M at a mole ratio of 1:1.3 resulted in site-specific labeling at C70 only, presumably due to the high exposure of F70C to the external aqueous environment and the buried environment around C208 (also bound to Zn^{2+}) within the active site, making F5M difficult to approach C208 (Figure 1b). When the mole ratio of F70C to F5M further increases to 1:3, fluorophore labeling at both C70 and C208 appears to occur (Figure 1c; molecular mass = 26490 Da). The measured molecular mass values of F70C and F70Cf are 25637 and 26064 Da, respectively, which are consistent with the calculated molecular mass values of F70C and F70Cf (25636 and 26063 Da, respectively, calculated by the Expasy program). Moreover, the mass difference between the labeled and unlabeled F70C mutants is consistent with the molecular mass of F5M (427 Da).

The labeling site of F70C was further studied by trypsin digestion of F70Cf analyzed by ESI-MS. After trypsin digestion, peptide fragments (Figure 2) including C208 and C70 were VFYPGPGHTSDNITVGIDGTDIAFGG**C**LIK (mass to charge ratio, m/z = 1022.1746) and QLAPNVWQHTSYLDMPG**C**GAVASNGLIVR (m/z = 1033.1849), respectively. Moreover, m/z values of digested peptide fragments including C208 and C70 with F5M were

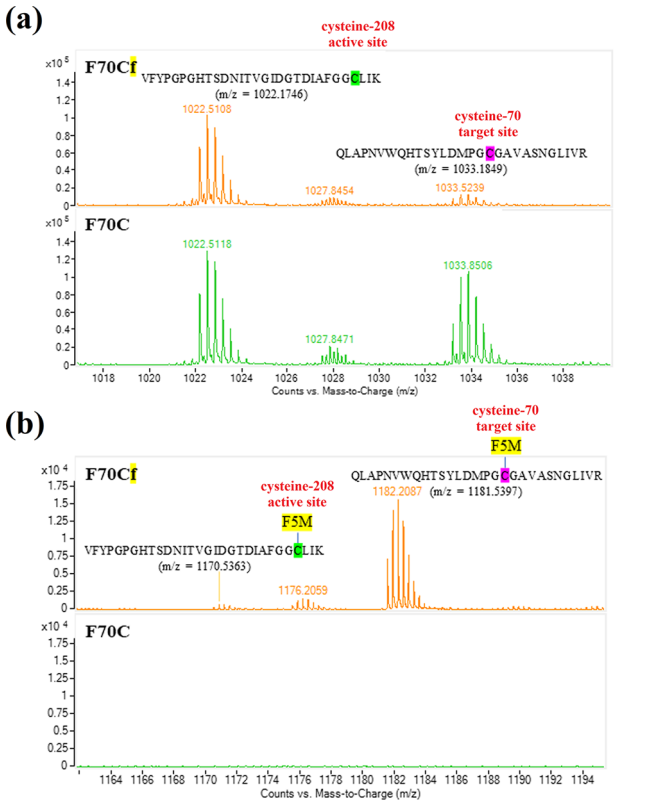

MEIRPTIGQQMETGDQRFGDLVFRQLAPNVWQHTS
YLDMPG**C**GAVASNGLIVRDGGRVLVVDTAWTDDQ
TAQILNWIKQEINLPVALAVVTHAHQDKMGGMDA
LHAAGIATYANALSNQLAPQEGMVAAQHSLTFAAN
GWVEPATAPNFGPLKVFYPGPGHTSDNITVGIDGTD
IAFGG**C**LIKDSKAKSLGNLGDADTEHYAASARAFG
AAFPKASMIVMSHSAPDSRAAITHTARMADKLR

Figure 2. ESI-MS spectra of trypsin-digested F70C and F70Cf. (a) The peptide fragment showing the amino acid sequence from the position of 53 to 81 (QLAPNVWQHTSYLDMPG**C**GAVASNGLIVR) with an m/z value of 1033.1849 indicates the position of cysteine-70 (target site, highlighted in purple), while the fragment showing the amino acid sequence from the position of 182 to 211 displays the position of cysteine-208 (active site, highlighted in green). (b) The m/z values of peptide fragments of cysteine-70 with F5M (highlighted in yellow) and cysteine-208 with F5M are 1181.5397 and 1170.5363, respectively.

1170.5363 and 1181.5397, respectively. The results proved that virtually all F5M was labeled at C70, as revealed by the dominant peak. Only a minor mass peak is associated with C208 attached to F5M (Figure 2).

Fluorescence Detection of β-Lactam Antibiotics. Fluorescent F70Cf can specifically respond to β-lactam antibiotics. When F70Cf is mixed with β-lactam antibiotics (cefotaxime and cephalothin), the fluorescence signals increase and then decrease gradually as a function of time (Figure 3a). Our previous studies have shown that binding of β-lactam antibiotics to the enzyme's active site induces the fluorophore to depart from the active site so that the fluorescein label (F5M) becomes well exposed to an external aqueous environment and/or stays away from amino acid quenchers in the active site.[24,25] When the antibiotic is hydrolyzed to the acid product, the fluorescein label (F5M) returns to the active

https://doi.org/10.1021/acsomega.3c08117
ACS Omega 2024, 9, 9161−9169

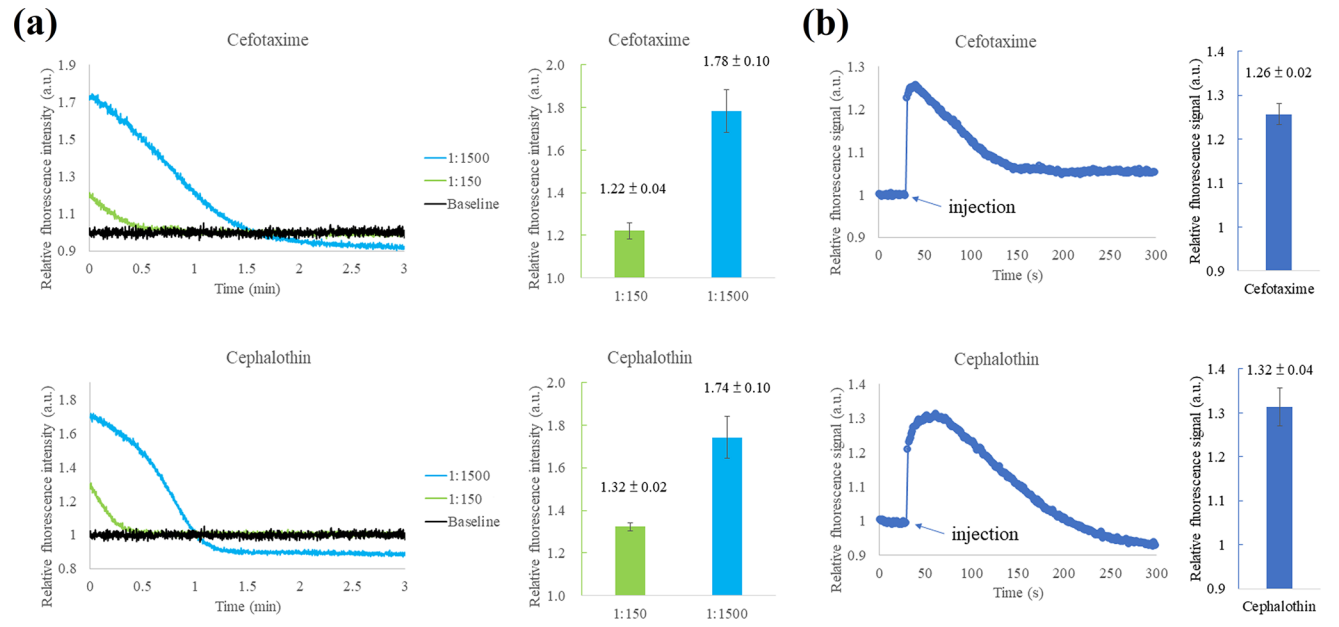

Figure 3. Fluorescence measurements of F70Cf with antibiotics. Time-course fluorescence and fluorescence microplate reader measurements of F70Cf with two β-lactam antibiotics, cefotaxime and cephalothin, are shown in panels (a) and (b), respectively. (a) For time-course fluorescence measurements, the mole ratios of F70Cf to cefotaxime and cephalothin antibiotics are 1:0 (black), 1:150 (green), and 1:1500 (blue). (b) For fluorescence microplate reader measurements, the molar ratio of F70Cf to cefotaxime and cephalothin antibiotics is 1:1500.

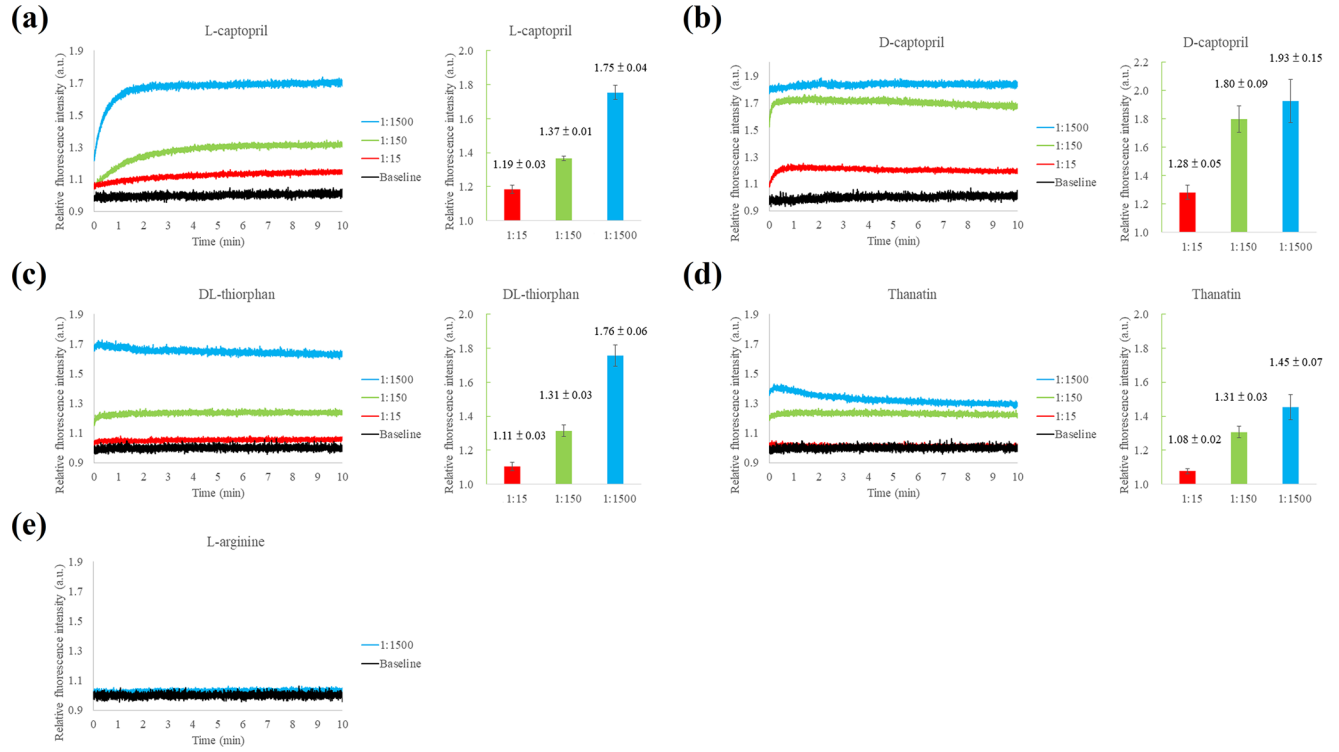

Figure 4. Time-course fluorescence measurements of F70Cf with various inhibitors. The fluorescence profiles for L-captopril, D-captopril, DL-thiorphan, thanatin, and L-arginine are shown in panels (a)−(e), respectively. The mole ratios of F70Cf to each inhibitor are 1:0 (black), 1:15 (red), 1:150 (green), and 1:1500 (blue).

site, thus restoring its weak fluorescence signal.[24,25] To demonstrate that fluorescent F70Cf is compatible with a high-throughput microplate reader, which is common in *in vitro* drug screening, F70Cf was placed on a microplate reader and injected with cefotaxime and cephalothin (Figure 3b). In both cases, the antibiotics cause F70Cf to give stronger fluorescence signals and then decline fluorescence signals as a function of time, similar to the results recorded with the spectrofluorometer (Figure 3a). These results indicate the capability of F70Cf in *in vitro* drug screening with a high-throughput microplate reader. Unlike another method that uses about 2−3 h to detect antibiotics by NDM-1,[28] F70Cf could detect antibiotics in just a few minutes and was more time-efficient.

https://doi.org/10.1021/acsomega.3c08117
ACS Omega 2024, 9, 9161−9169

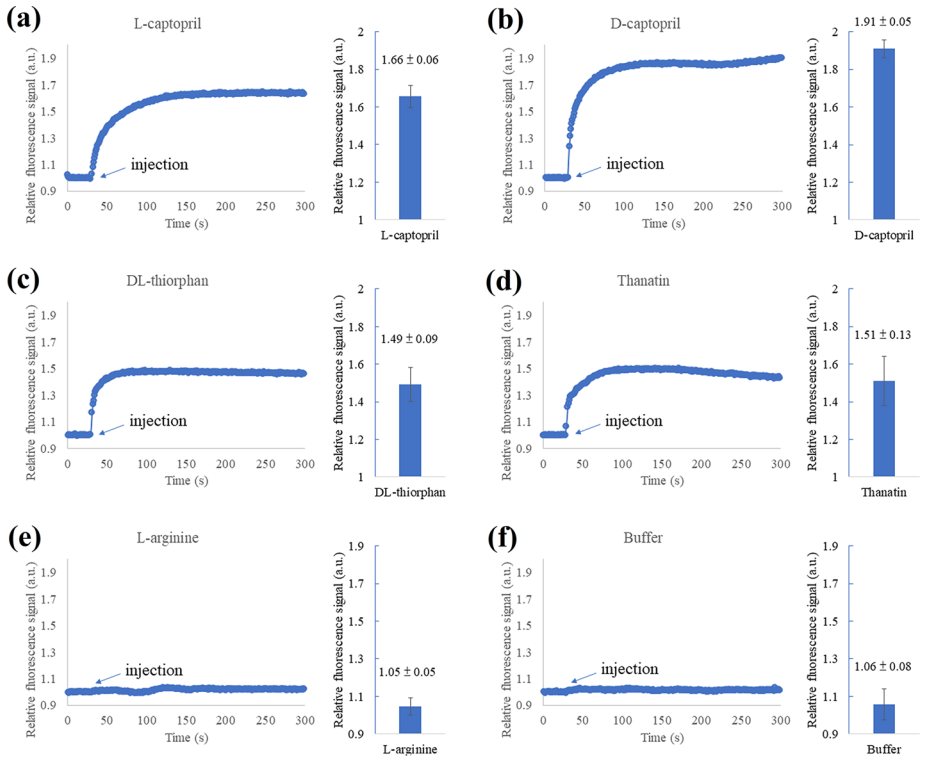

Figure 5. Fluorescence measurements of F70Cf with various inhibitors using a fluorescence microplate reader. The fluorescence profiles for L-captopril, D-captopril, DL-thiorphan, thanatin, L-arginine, and 50 μM $ZnCl_2$ and 20 mM Tris−HCl buffer (pH 7.0) are shown in panels (a)−(f), respectively. The mole ratio of F70Cf to each inhibitor is 1:1500.

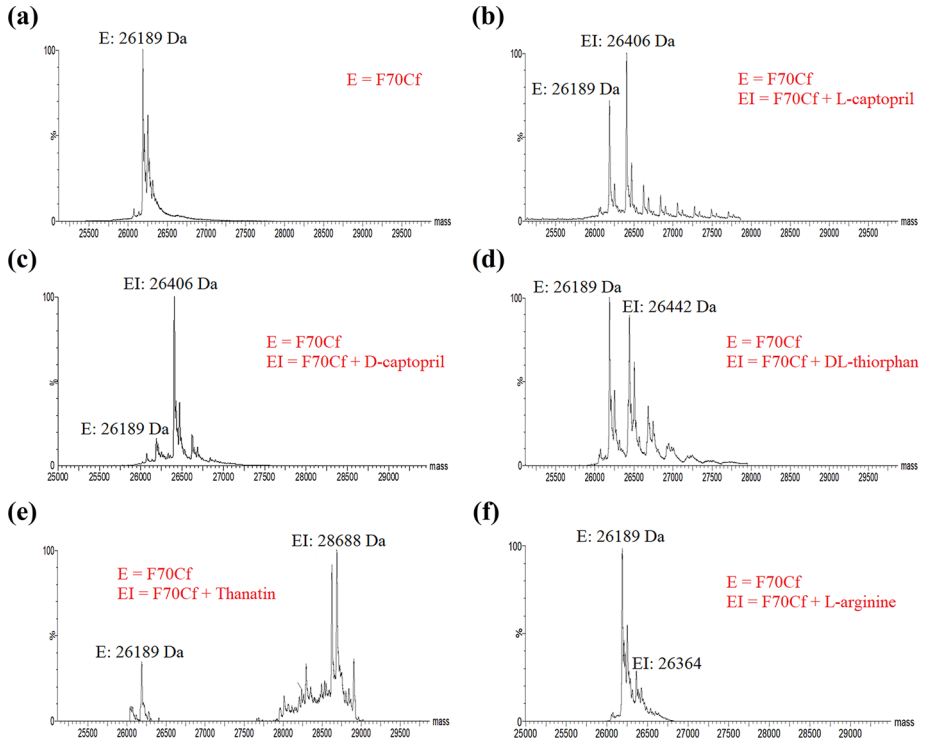

Figure 6. Binding studies of F70Cf with different inhibitors by native ESI-MS. The molecular mass of F70Cf in its native state was measured to be 26189 Da (a). The binding profiles for L-captopril, D-captopril, DL-thiorphan, thanatin, and L-arginine are shown in panels (b)−(f), respectively.

Fluorescence Detection of Non-β-Lactam Inhibitors. We then studied the ability of fluorescent F70Cf to detect non-β-lactam inhibitors (L-captopril, D-captopril, DL-thiorphan, and thanatin),[29−37] which are able to bind to NDM-type β-lactamases. As shown in Figure 4, the fluorescence signals of F70Cf increase with the dose of the inhibitors (Figure 4). The sustained fluorescence increases imply that the inhibitors continuously occupy the active site of F70Cf. Among the

https://doi.org/10.1021/acsomega.3c08117
ACS Omega 2024, 9, 9161−9169

inhibitors, L-captopril shows a gradual increase in fluorescence in the initial phase, whereas D-captopril, DL-thiorphan, and thanatin virtually do not (Figure 4a–d). These findings indicate that D-captopril, DL-thiorphan, and thanatin bind much faster to F70Cf as compared to L-captopril (Figure 4a–d). To trace the initial binding phases of the fast inhibitors (D-captopril, DL-thiorphan, and thanatin), we used a microplate reader to monitor the fluorescence signals as a function of time. As shown in Figure 5a–d, the initial increases in fluorescence signal for D-captopril, DL-thiorphan, and thanatin are much faster than those for L-captopril, implying that D-captopril, DL-thiorphan, and thanatin are likely to have higher binding affinity to F70Cf compared to L-captopril. These results are consistent with the IC_{50} values of these inhibitors to NDM-1; the IC_{50} values of L-captopril, D-captopril, DL-thiorphan, and thanatin were found to be 157.4,[29] 20.1,[29] 1.8,[36] and 3.21 μM,[37] respectively. These observations reveal that F70Cf is capable of screening for noncovalent small molecules/peptides *in vitro*. To verify that F70Cf is specific to active-site binders only, we performed control experiments with buffer and L-arginine (Figures 4e and 5e,f). In both cases, F70Cf shows no significant fluorescence changes with these nonbinders (Figures 4e and 5e,f).

Studies of Binding Interactions of F70Cf with Inhibitors by Native Mass Spectrometry. To further verify that F70Cf can bind to the non-β-lactam inhibitors noncovalently, native ESI-MS measurements were performed. Figure 6 shows the ESI mass spectra of F70Cf with the inhibitors, where E and EI represent the F70Cf and F70Cf–inhibitor complexes, respectively. In general, the inhibitors can form noncovalent complexes with F70Cf in a significant population, whereas the nonbinder L-arginine virtually cannot form an F70Cf–L-arginine complex in a significant population. These results support the fact that the fluorescence enhancements of F70Cf with the inhibitors arise from the binding of the inhibitors to the active site (Figures 4a–d and 5a–d).

Molecular Modeling of F70Cf with Inhibitors. The mechanism of F70Cf fluorescence enhancement after binding to inhibitors was investigated by molecular modeling. F70Cf has the fluorophore-labeled C70 side chain (in gray) buried and occupying the substrate-binding site, which experiences a hydrophobic environment that may also contain amino acid quenchers, resulting in a weaker fluorescence signal (Figure 7a). When L-captopril (orange sticks) binds to the F70Cf active site, it displaces the fluorescein label attached to C70 into the external aqueous environment (now shown in bright green), leading to a stronger fluorescence signal (Figure 7b). When thanatin (orange cartoon, Figure 7c) and cefotaxime (orange cartoon, Figure 7d) bind to F70Cf's active site, they also displace the C70f-labeled side chain (bright green) into the solvent and lead to a stronger fluorescence signal (Figure 7c,d). To confirm the molecular modeling results, a proteolytic study on F70Cf was performed. After 1–18 h of trypsin digestion, digested fragments with the fluorescein label are exposed to the external aqueous environment, leading to an increase in fluorescence in a time-dependent manner (Figure 7e). These findings are consistent with the molecular modeling results.

CONCLUSIONS

We have successfully constructed a fluorescent drug sensor from NDM-1 through structural analysis, protein engineering, and fluorophore labeling that is capable of sensing β-lactam antibiotics and non-β-lactam inhibitors. This functional drug sensor can identify impotent β-lactam antibiotics by exhibiting characteristic fluorescence profiles (an increasing fluorescence signal in the initial phase due to antibiotic binding followed by a declining signal as a result of β-lactam hydrolysis to the acid product). Upon binding to non-β-lactam inhibitors (L-captopril, D-captopril, DL-thiorphan, and thanatin), the NDM-1 drug sensor gives stronger and sustained fluorescence signals. These exciting results highlight the great potential of the fluorescent NDM-1 drug sensor in *in vitro* drug screening for potent inhibitors. More importantly, our study of the fluorescent NDM-1 drug sensor has paved the way to further develop a class of tailor-made fluorescent drug sensors from clinically significant NDM-type variants to search for potent

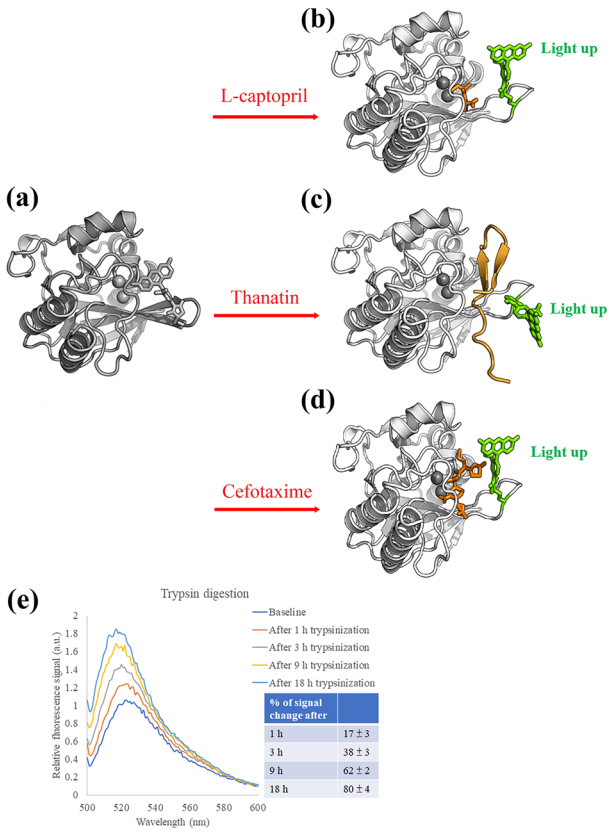

Figure 7. Molecular models of F70Cf with inhibitors. (a) The F70Cf fluorophore-labeled at the C70f side chain is indicated in gray. The model was created with Coot and JLigand, both of the CCP4 suite.[38,39] (b) The complex of F70Cf with L-captopril (orange sticks) enhanced the fluorescence signal (bright green). (c) The complex of F70Cf with thanatin (orange cartoon) enhanced the fluorescence signal (bright green). (d) The complex of F70Cf with cefotaxime (orange cartoon) enhanced the fluorescence signal (bright green). (e) Fluorescence spectra of F70Cf in the presence of trypsin were recorded at different time intervals. The protein traces are shown as cartoon models (gray), with zinc ions as spheres. The apo model was constructed from PDB ID 3SPU (B chain),[40] whereas the L-captopril complex was from PDB ID 4EXS (B chain).[34] The NDM-1:thanatin complex was created with the help of ColabFold ("AlphaFold2 with MMSeq2" notebook using the "PDB70" template).[41] The model with cefotaxime was built with Coot, referencing PDB ID 4RL0,[17] the structure of NDM-1 with hydrolyzed cefuroxime. The R2 group of cefotaxime was grafted from the corresponding fragment of substrate in PDB ID 6C79.[42] The figures were created with PyMOL. Photograph courtesy of Yu Wai Chen. Copyright 2024 (panels a–d).

https://doi.org/10.1021/acsomega.3c08117
ACS Omega 2024, 9, 9161–9169

and new inhibitors. Such work is particularly important to fight against superbugs acquiring NDM-type β-lactamases.

■ ASSOCIATED CONTENT

Supporting Information

The Supporting Information is available free of charge at https://pubs.acs.org/doi/10.1021/acsomega.3c08117.

SDS-PAGE analysis, molecular mass, secondary structure, and specific activities of WT-NDM-1, F70C, and F70Cf (PDF)

■ AUTHOR INFORMATION

Corresponding Authors

Kwok-Yin Wong − *State Key Laboratory of Chemical Biology and Drug Discovery, Department of Applied Biology and Chemical Technology, The Hong Kong Polytechnic University, Hong Kong, China;* orcid.org/0000-0003-4984-7109; Email: kwok-yin.wong@polyu.edu.hk

Yun-Chung Leung − *State Key Laboratory of Chemical Biology and Drug Discovery, Department of Applied Biology and Chemical Technology and Lo Ka Chung Research Centre for Natural Anti-Cancer Drug Development, The Hong Kong Polytechnic University, Hong Kong, China;* orcid.org/0000-0003-3590-7027; Email: thomas.yun-chung.leung@polyu.edu.hk

Authors

Sai-Fung Chung − *State Key Laboratory of Chemical Biology and Drug Discovery, Department of Applied Biology and Chemical Technology and Lo Ka Chung Research Centre for Natural Anti-Cancer Drug Development, The Hong Kong Polytechnic University, Hong Kong, China*

Suet-Ying Tam − *State Key Laboratory of Chemical Biology and Drug Discovery, Department of Applied Biology and Chemical Technology and Lo Ka Chung Research Centre for Natural Anti-Cancer Drug Development, The Hong Kong Polytechnic University, Hong Kong, China*

Wai-Ting Wong − *State Key Laboratory of Chemical Biology and Drug Discovery, Department of Applied Biology and Chemical Technology, The Hong Kong Polytechnic University, Hong Kong, China*

Pui-Kin So − *State Key Laboratory of Chemical Biology and Drug Discovery, Department of Applied Biology and Chemical Technology, The Hong Kong Polytechnic University, Hong Kong, China*

Wing-Lam Cheong − *Department of Science, School of Science and Technology, Hong Kong Metropolitan University, Hong Kong, Hong Kong*

Chun-Wing Mak − *State Key Laboratory of Chemical Biology and Drug Discovery, Department of Applied Biology and Chemical Technology, The Hong Kong Polytechnic University, Hong Kong, China*

Leo Man-Yuen Lee − *State Key Laboratory of Chemical Biology and Drug Discovery, Department of Applied Biology and Chemical Technology, The Hong Kong Polytechnic University, Hong Kong, China*

Pak-Ho Chan − *State Key Laboratory of Chemical Biology and Drug Discovery, Department of Applied Biology and Chemical Technology, The Hong Kong Polytechnic University, Hong Kong, China*

Complete contact information is available at: https://pubs.acs.org/10.1021/acsomega.3c08117

Author Contributions

#S.-F.C. and S.-Y.T. contributed equally to this work.

Funding

The General Research Fund (GRF) project no. PolyU 151069/17M (RGC reference number 15106917), The Hong Kong Polytechnic University and the State Key Laboratory of Chemical Biology and Drug Discovery (K-BBX4), Postdoc Matching Fund Scheme (P0035831/1-W17P), Lo Ka Chung Charitable Foundation endowed professorship in pharmaceutical sciences, and Patrick S. C. Poon endowed professorship.

Notes

The authors declare no competing financial interest.

■ ACKNOWLEDGMENTS

We would like to thank Dr. Yu Wai Chen for constructing the molecular modeling.

■ ABBREVIATIONS

NDM-1, New Delhi metallo-β-lactamase-1; PBP, penicillin-binding proteins; ESI-MS, electrospray ionization−mass spectrometry

■ REFERENCES

(1) Palacios, A. R.; Rossi, M. A.; Mahler, G. S.; Vila, A. J. Metallo-beta-Lactamase Inhibitors Inspired on Snapshots from the Catalytic Mechanism. *Biomolecules* **2020**, *10* (6), 854.

(2) CDC *Antibiotic Resistance Threats in the United States*. U.S. Department of Health and Human Services 2019.

(3) Fisher, J. F.; Meroueh, S. O.; Mobashery, S. Bacterial Resistance to beta-Lactam Antibiotics: Compelling Opportunism, Compelling Opportunity. *Chem. Rev.* **2005**, *105* (2), 395−424.

(4) Bush, K.; Bradford, P. A. β-Lactams and β-Lactamase Inhibitors: An Overview. *Cold Spring Harbor Perspect. Med.* **2016**, *6* (8), a025247.

(5) Bush, K. The ABCD's of Beta-Lactamase Nomenclature. *J. Infect Chemother* **2013**, *19* (4), 549−59.

(6) Matagne, A.; Lamotte-Brasseur, J.; Frère, J. M. Catalytic Properties of Class A Beta-lactamases: Efficiency and Diversity. *Biochem. J.* **1998**, *330* (Pt 2), 581−98.

(7) Matagne, A.; Dubus, A.; Galleni, M.; Frere, J. M. The Beta-lactamase Cycle: a Tale of Selective Pressure and Bacterial Ingenuity. *Nat. Prod Rep* **1999**, *16* (1), 1−19.

(8) Boyd, S. E.; Livermore, D. M.; Hooper, D. C.; Hope, W. W. Metallo-beta-Lactamases: Structure, Function, Epidemiology, Treatment Options, and the Development Pipeline. *Antimicrob. Agents Chemother.* **2020**, *64* (10), 10.

(9) Ventola, C. L. The Antibiotic Resistance Crisis: Part 1: Causes and Threats. *P T* **2015**, *40* (4), 277−83.

(10) Mojica, M. F.; Rossi, M. A.; Vila, A. J.; Bonomo, R. A. The Urgent Need for Metallo-beta-Lactamase Inhibitors: an Unattended Global Threat. *Lancet Infect Dis* **2022**, *22* (1), e28−e34.

(11) Bi, R.; Kong, Z.; Qian, H.; Jiang, F.; Kang, H.; Gu, B.; Ma, P. High Prevalence of bla NDM Variants Among Carbapenem-Resistant Escherichia coli in Northern Jiangsu Province China. *Front. Microbiol.* **2018**, *9*, 2704.

(12) Nordmann, P.; Boulanger, A. E.; Poirel, L. NDM-4 Metallo-beta-Lactamase with Increased Carbapenemase Activity from Escherichia Coli. *Antimicrob. Agents Chemother.* **2012**, *56* (4), 2184−6.

(13) Cheng, Z.; Thomas, P. W.; Ju, L.; Bergstrom, A.; Mason, K.; Clayton, D.; Miller, C.; Bethel, C. R.; VanPelt, J.; Tierney, D. L.; Page, R. C.; Bonomo, R. A.; Fast, W.; Crowder, M. W. Evolution of New Delhi Metallo-beta-Lactamase (NDM) in the Clinic: Effects of NDM Mutations on Dtability, Zinc Affinity, and Mono-Zinc Activity. *J. Biol. Chem.* **2018**, *293* (32), 12606−12618.

(14) Kumarasamy, K. K.; Toleman, M. A.; Walsh, T. R.; Bagaria, J.; Butt, F.; Balakrishnan, R.; Chaudhary, U.; Doumith, M.; Giske, C. G.; Irfan, S.; Krishnan, P.; Kumar, A. V.; Maharjan, S.; Mushtaq, S.; Noorie, T.; Paterson, D. L.; Pearson, A.; Perry, C.; Pike, R.; Rao, B.; Ray, U.; Sarma, J. B.; Sharma, M.; Sheridan, E.; Thirunarayan, M. A.; Turton, J.; Upadhyay, S.; Warner, M.; Welfare, W.; Livermore, D. M.; Woodford, N. Emergence of a New Antibiotic Resistance Mechanism in India, Pakistan, and the UK: a Molecular, Biological, and Epidemiological Study. *Lancet Infect Dis* **2010**, *10* (9), 597−602.
(15) Dai, T.; Xiao, Z.; Shan, D.; Moreno, A.; Li, H.; Prakash, M.; Banaei, N.; Rao, J. Culture-Independent Multiplexed Detection of Drug-Resistant Bacteria Using Surface-Enhanced Raman Scattering. *ACS Sens* **2023**, *8* (8), 3264−3271.
(16) Bahr, G.; Vitor-Horen, L.; Bethel, C. R.; Bonomo, R. A.; Gonzalez, L. J.; Vila, A. J. Clinical Evolution of New Delhi Metallo-β-Lactamase (NDM) Optimizes Resistance under Zn(II) Deprivation. *Antimicrob. Agents Chemother.* **2018**, *62* (1), No. e01849-17.
(17) Feng, H.; Ding, J.; Zhu, D.; Liu, X.; Xu, X.; Zhang, Y.; Zang, S.; Wang, D. C.; Liu, W. Structural and Mechanistic Insights into NDM-1 Catalyzed Hydrolysis of Cephalosporins. *J. Am. Chem. Soc.* **2014**, *136* (42), 14694−7.
(18) Zhang, H.; Hao, Q. Crystal Structure of NDM-1 Reveals a Common beta-Lactam Hydrolysis Mechanism. *Faseb J.* **2011**, *25* (8), 2574−82.
(19) Thomas, P. W.; Zheng, M.; Wu, S.; Guo, H.; Liu, D.; Xu, D.; Fast, W. Characterization of Purified New Delhi Metallo-beta-Lactamase-1. *Biochemistry* **2011**, *50* (46), 10102−13.
(20) Cheong, W. L.; Tsang, M. S.; So, P. K.; Chung, W. H.; Leung, Y. C.; Chan, P. H. Fluorescent TEM-1 beta-Lactamase with Wild-Type Activity as a Rapid Drug Sensor for In Vitro Drug Screening. *Biosci. Rep.* **2014**, *34* (5), No. e00136.
(21) Hu, R.; Yap, H. K.; Fung, Y. H.; Wang, Y.; Cheong, W. L.; So, L. Y.; Tsang, C. S.; Lee, L. Y.; Lo, W. K.; Yuan, J.; Sun, N.; Leung, Y. C.; Yang, G.; Wong, K. Y. 'Light Up' Protein-Protein Interaction Through Bioorthogonal Incorporation of a Turn-on Fluorescent Probe into beta-Lactamase. *Mol. Biosyst* **2016**, *12* (12), 3544−3549.
(22) Wong, W. T.; Chan, K. C.; So, P. K.; Yap, H. K.; Chung, W. H.; Leung, Y. C.; Wong, K. Y.; Zhao, Y. Increased Structural Flexibility at the Active Site of a Fluorophore-Conjugated beta-Lactamase Distinctively Impacts its Binding toward Diverse Cephalosporin Antibiotics. *J. Biol. Chem.* **2011**, *286* (36), 31771−80.
(23) Tam, S. Y.; Chung, S. F.; Chen, Y. W.; So, Y. H.; So, P. K.; Cheong, W. L.; Wong, K. Y.; Leung, Y. C. Design of a structure-based fluorescent biosensor from bioengineered arginine deiminase for rapid determination of L-arginine. *Int. J. Biol. Macromol.* **2020**, *165* (Pt A), 472−482.
(24) Chan, P. H.; So, P. K.; Ma, D. L.; Zhao, Y.; Lai, T. S.; Chung, W. H.; Chan, K. C.; Yiu, K. F.; Chan, H. W.; Siu, F. M.; Tsang, C. W.; Leung, Y. C.; Wong, K. Y. Fluorophore-Labeled beta-Lactamase as a Biosensor for beta-Lactam Antibiotics: a Study of the Biosensing Process. *J. Am. Chem. Soc.* **2008**, *130* (20), 6351−61.
(25) Tsang, M. W.; Chan, P. H.; So, P. K.; Ma, D. L.; Tsang, C. W.; Wong, K. Y.; Leung, Y. C. Engineered Amp C beta-Lactamase as a Fluorescent Screening Tool for Class C beta-Lactamase Inhibitors. *Anal. Chem.* **2011**, *83* (6), 1996−2004.
(26) Green, V. L.; Verma, A.; Owens, R. J.; Phillips, S. E. V.; Carr, S. B. Structure of New Delhi Metallo-beta-Lactamase 1 (NDM-1). *Acta Crystallogr. Sect. F: Struct. Biol. Cryst. Commun.* **2011**, *67* (Pt 10), 1160−4.
(27) Yang, H.; Aitha, M.; Marts, A. R.; Hetrick, A.; Bennett, B.; Crowder, M. W.; Tierney, D. L. Spectroscopic and Mechanistic Studies of Heterodimetallic Forms of Metallo-beta-Lactamase NDM-1. *J. Am. Chem. Soc.* **2014**, *136* (20), 7273−85.
(28) Meng, Q.; Wang, Y.; Long, Y.; Yue, A.; Mecklenburg, M.; Tian, S.; Fu, Y.; Yao, X.; Liu, J.; Song, D.; Wu, C.; Xie, B. Rapid Detection of Multiple Classes of beta-Lactam Antibiotics in Blood Using an NDM-1 Biosensing Assay. *Antibiotics* **2021**, *10* (9), 1110.
(29) Brem, J.; van Berkel, S. S.; Zollman, D.; Lee, S. Y.; Gileadi, O.; McHugh, P. J.; Walsh, T. R.; McDonough, M. A.; Schofield, C. J. Structural Basis of Metallo-beta-Lactamase Inhibition by Captopril Stereoisomers. *Antimicrob. Agents Chemother.* **2016**, *60* (1), 142−50.
(30) Li, N.; Xu, Y.; Xia, Q.; Bai, C.; Wang, T.; Wang, L.; He, D.; Xie, N.; Li, L.; Wang, J.; Zhou, H. G.; Xu, F.; Yang, C.; Zhang, Q.; Yin, Z.; Guo, Y.; Chen, Y. Simplified Captopril Analogues as NDM-1 Inhibitors. *Bioorg. Med. Chem. Lett.* **2014**, *24* (1), 386−9.
(31) Rydzik, A. M.; Brem, J.; van Berkel, S. S.; Pfeffer, I.; Makena, A.; Claridge, T. D.; Schofield, C. J. Monitoring Conformational Changes in the NDM-1 Metallo-beta-Lactamase by 19F NMR Spectroscopy. *Angew. Chem., Int. Ed. Engl.* **2014**, *53* (12), 3129−33.
(32) Linciano, P.; Cendron, L.; Gianquinto, E.; Spyrakis, F.; Tondi, D. Ten Years with New Delhi Metallo-beta-lactamase-1 (NDM-1): From Structural Insights to Inhibitor Design. *ACS Infect Dis* **2019**, *5* (1), 9−34.
(33) Wang, T.; Xu, K.; Zhao, L.; Tong, R.; Xiong, L.; Shi, J. Recent Research and Development of NDM-1 Inhibitors. *Eur. J. Med. Chem.* **2021**, *223*, No. 113667.
(34) King, D. T.; Worrall, L. J.; Gruninger, R.; Strynadka, N. C. New Delhi Metallo-beta-Lactamase: Structural Insights into beta-Lactam Recognition and Inhibition. *J. Am. Chem. Soc.* **2012**, *134* (28), 11362−5.
(35) Ma, G.; Wang, S.; Wu, K.; Zhang, W.; Ahmad, A.; Hao, Q.; Lei, X.; Zhang, H. Structure-Guided Optimization of D-captopril for Discovery of Potent NDM-1 Inhibitors. *Bioorg. Med. Chem.* **2021**, *29*, No. 115902.
(36) Klingler, F. M.; Wichelhaus, T. A.; Frank, D.; Cuesta-Bernal, J.; El-Delik, J.; Muller, H. F.; Sjuts, H.; Gottig, S.; Koenigs, A.; Pos, K. M.; Pogoryelov, D.; Proschak, E. Approved Drugs Containing Thiols as Inhibitors of Metallo-beta-lactamases: Strategy To Combat Multidrug-Resistant Bacteria. *J. Med. Chem.* **2015**, *58* (8), 3626−30.
(37) Ma, B.; Fang, C.; Lu, L.; Wang, M.; Xue, X.; Zhou, Y.; Li, M.; Hu, Y.; Luo, X.; Hou, Z. The Antimicrobial Peptide Thanatin Disrupts the Bacterial Outer Membrane and Inactivates the NDM-1 Metallo-beta-Lactamase. *Nat. Commun.* **2019**, *10* (1), 3517.
(38) Emsley, P.; Lohkamp, B.; Scott, W. G.; Cowtan, K. Features and Development of Coot. *Acta Crystallogr., Sect. D: Biol. Crystallogr.* **2010**, *66* (Pt 4), 486−501.
(39) Lebedev, A. A.; Young, P.; Isupov, M. N.; Moroz, O. V.; Vagin, A. A.; Murshudov, G. N. JLigand: a Graphical Tool for the CCP4 Template-Restraint Library. *Acta Crystallogr. D Biol. Crystallogr.* **2012**, *68* (Pt 4), 431−40.
(40) King, D.; Strynadka, N. Crystal Structure of New Delhi Metallo-Beta-Lactamase Reveals Molecular Basis for Antibiotic Resistance. *Protein Sci.* **2011**, *20* (9), 1484−91.
(41) Mirdita, M.; Schutze, K.; Moriwaki, Y.; Heo, L.; Ovchinnikov, S.; Steinegger, M. ColabFold: Making Protein Folding Accessible to All. *Nat. Methods* **2022**, *19* (6), 679−682.
(42) Langan, P. S.; Vandavasi, V. G.; Cooper, S. J.; Weiss, K. L.; Ginell, S. L.; Parks, J. M.; Coates, L. Substrate Binding Induces Conformational Changes in a Class A Beta-lactamase That Prime It for Catalysis. *ACS Catal.* **2018**, *8*, 2428−2437.

https://doi.org/10.1021/acsomega.3c08117
ACS Omega 2024, 9, 9161−9169